Polymer 244 (2022) 124561

Contents lists available at ScienceDirect

Polymer

journal homepage: www.elsevier.com/locate/polymer

Study on the effects of soluble POSS on chain disentanglement in UHMWPE polymerization

Jian Zhou [a], Xian Zhang [a], Shicheng Zhao [a], Chunlin Ye [a], Zhenfei Zhang [b], Shiao-Wei Kuo [c], Zhong Xin [a,*]

[a] Shanghai Key Laboratory of Multiphase Materials Chemical Engineering, Department of Product Engineering, East China University of Science and Technology, Shanghai, 200237, People's Republic of China
[b] State Key Laboratory of Polyolefins and Catalysis, Shanghai Key Laboratory of Catalysis Technology for Polyolefins (Shanghai Research Institute of Chemical Industry), Shanghai, 200062, China
[c] Department of Materials and Optoelectronic Science, National Sun Yat-Sen University, Kaohsiung, 804, Taiwan

ARTICLE INFO

Keywords:
POSS/UHMWPE composite
Melt viscosity
In-situ polymerization

ABSTRACT

Polyhedral oligomeric silsesquioxanes (POSS) was added in ultrahigh molecular weight polyethylene (UHMWPE) to intercalate the molecular network and produce chain disentanglement. To avoid agglomeration, the POSS/UHMWPE composites were prepared by in-situ polymerization. In particular, POSS used in this experiment is soluble in the polymerization process, so it can be dispersed in the form of nm-scale in UHMWPE. The reduced melt viscosity and the increased molecular weight between entanglement (M_e) revealed that the addition of POSS can induce the disentanglement of UHMWPE and the optimal content is 0.2 wt%. The isothermal and non-isothermal crystallization behavior of nanocomposites were studied by a differential scanning calorimetry (DSC). The crystallization rate and the crystallinity of UHMWPE increased with the addition of POSS, indicating that POSS could act as a nucleating agent in UHMWPE. The annealing study was carried out by a Flash DSC and two melting peaks were observed. The data was analyzed by Arrhenius equation and the POSS/UHMWPE was found to have a lower melting activation energy than neat UHMWPE, proving the disentanglement effect of POSS on UHMWPE.

1. Introduction

Ultrahigh molecular weight polyethylene (UHMWPE) is an ultra-modern engineering material with a molecular weight over 10^6 g/mol as defined by ISO 11542 [1]. It is represented as a semi-crystalline polymer consisting of orthogonal crystalline phase, amorphous phase and mesophase [2]. The crystalline phase is made of ordered macromolecules while the amorphous region consists of loops, entangled chains and tie molecules [3]. The chain diffusion, chain dynamics, crystalline order and melt viscoelasticity of semi-crystal polymers are controlled by the topological constraints (entanglements) in the amorphous regions [4–6]. The large number of entanglements caused by the ultrahigh molecular weight brings both excellent mechanical properties and high melt viscosity which causes difficulty in manufacturing and multiple crystal defects during processing. Recent developments of disentanglements of UHMWPE have attracted much attention. Rastogi et al. [7] carried out polymerization with heterogeneous catalysts and discovered that low-temperature and low catalyst concentration could improve the regularity of chain segment. Li et al. [8–10] designed novel catalysts with rigid particles loaded on the carriers. The active centers were cut off and the synthesized UHMWPE had a lower melting viscosity.

In addition to disentangling UHMWPE during polymerization, nanoparticles can intercalate the molecular network to adjust their macroscopic and microscopic properties [11]. The investigation of the crystallization of UHMWPE with reduced Graphene Oxide Nanoplates (rGON) revealed that with the addition of suitable filler, chain segment can be retained in the nonequilibrium melt state of lower entanglement density [12]. Polyhedral oligomeric silsesquioxanes (POSS) is a kind of rigid particles with adjustable substituents [13]. It is estimated as the minimum silica grain with a specific size of 1.5 nm, which is equivalent to the segment and coil size of most polymers [14,15]. Adding POSS as the filler to disentangle polymers has been discussed recently [16–19]. However, POSS tends to agglomerate during blending, thus affecting the additive effect of nanomaterials.

* Corresponding author.
E-mail address: xzh@ecust.edu.cn (Z. Xin).

https://doi.org/10.1016/j.polymer.2022.124561
Received 21 November 2021; Received in revised form 11 January 2022; Accepted 16 January 2022
Available online 18 January 2022

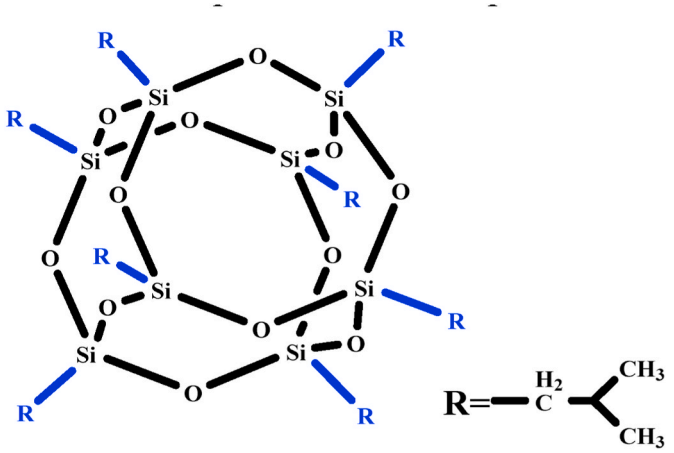

Scheme 1. Structure of Octaisobutyl-POSS.

In-situ polymerization has been reported to be an effective method to alleviate the agglomeration of nanoparticles [20]. Angel [21] prepared disentangled waterborne acrylic/TiO_2 nanocomposites with outstanding properties by in-situ emulsion polymerization. Rong et al. [22] prepared a novel PE/palygorskite composites with improved properties resulting from good dispersion and strong interaction between the filler and the polymer matrix. Overall, the nanoparticles get a better dispersion by in-situ polymerization than conventional mixing, and the former product usually has better properties [23].

In this section, in-situ polymerization of UHMWPE was carried out to explore the effects of POSS on UHMWPE disentanglement. In view of previous studies, Octaisobutyl-POSS was chosen. Its size is about 1.5 nm, smaller than the tube size of UHMWPE. Compared with octmethyl-POSS we studied before, its dispersion was achieved not only by mechanical stirring. It is soluble in the UHMWPE polymerization, revealing that it can disperse in UHMWPE in the form of a single molecule. POSS was expected to intercalate the chains to disentangle the polymer and reduce the melt viscosity. Small amplitude oscillatory shear rheometer and DMA were applied to evaluate the degree of disentanglement qualitatively and quantitatively. DSC was utilized to study the melt and crystallization behavior of UHMWPE. Fast differential scanning calorimeter (Flash-DSC) was applied for the study of annealing-recrystallization behavior of UHMWPE. Via Arrhenius equation, the melting activation energy of UHMWPE was obtained. Thus, the chain slippage capacity of UHMWPE can be obtained quantitatively.

2. Experimental

2.1. Materials

In this section, the octaisobutyl-POSS (Scheme 1) was purchased from Forsman (Beijing) and was vacuum heated before use. The polymerization of UHMWPE was carried out with Ziegler-Natta catalyst, purified hexane and triethyl aluminum (TEA) provided by Shanghai Research Institute of Chemical Industry. The polymerization was carried out under anhydrous and oxygen-free conditions. Decahydronaphthalene for the test of ubbelohde viscometer was acquired from Sinopharm Chemical Reagent Co., Ltd.

2.2. Preparation of POSS/UHMWPE composites

A 2 L autoclave reactor pressurized with nitrogen was used for polymerization. Before the reaction, the reactor was kept at 110 °C in vacuum for 2 h and then refrigerated to room temperature. Some amount of POSS and 0.40 ml TEA were dissolved in 1 L purified hexane. Then the mixture and 30 mg catalyst were added into the reactor. All the operations were performed in a nitrogen atmosphere without oxygen and water. The polymerization was conducted under 0.6 MPa of ethylene with continued stirring (20 rpm).

Table 1
Conditions for the preparation of testing samples.

Test	Time of hot pressing/ min	Time of Cooling pressing/ min
Rotary rheometer	10	10
DMA	30	10
Mechanical properties test	45	10

2.3. Preparation of UHMWPE strips for test

The strips of UHMWPE for analysis were prepared by compression molding. The conditions of different strips are shown in Table 1. The manufacturing pressure was 10 kPa and the temperature was 210 °C.

2.4. Characterizations

2.4.1. Rotary rheometer

The degree of polymer entanglements was assessed by a rotary rheometer (MCR 302, Anton Paar, Austria). A plate of 8 mm (PP08) was utilized for the shear measurement, and the sample is 8 mm in diameter and 1 mm in thickness. The device was maintained at 180 °C for 5 min before the test to make sure that the test environment was stable. The frequency was from 100 to 0.01 rad s^{-1}. The measurement was operated at a constant strain of 0.25%, a temperature of 180 °C, a normal force of 0.25 N and under industrial N_2 atmosphere of 750 ml/h.

2.4.2. Dynamic mechanical analysis (DMA)

A DMA 1 profiler (Mettler Toledo, Switzerland) performed in tensile mode was used to estimate the entanglement of the samples (size: 20*10*2 mm^3). The measurement mode: fixed shifting of 10 mm, frequency of 1 Hz and temperature from 30 to 200 °C at the rate of 3 °C/min.

2.4.3. Ubbelohde viscometer

The viscosity molecular weight (Mv) of UHMWPE was measured by a ubbelohde viscometer. The samples were prepared as below: 10 mg nascent UHMWPE and 40 mg antioxidant were dissolved in 50 ml decahydronaphthalene. The mixture was kept at 150 °C for at least 4 h and then cooled to 135 °C for the measurement. The intrinsic viscosity and molecular were obtained by calculating the flow time of a given volume of the mixture through the capillary tube according to the equations below [24].

$$\eta = \frac{\left(\frac{2t_1}{t_0} - 2 - 2\ln\frac{t_1}{t_0}\right)^{0.5} * 500}{m} \quad (1)$$

$$M_v = 53700 * \eta^{1.37} \quad (2)$$

Among them, t_0 (s) is the flow time of pure decahydronaphthalene, t_1 (s) is the flow time of decahydronaphthalene with POSS/UHMWPE, and m (mg) is the mass of POSS/UHMWPE. Each sample should be measured 3 times.

2.4.4. Gel permeation chromatography (GPC)

A GPC instrument was utilized for the measurement of the molecular weight distribution (MWD) of POSS/UHMWPE composites according to ASTM D6474-1999(2006) and a flash column (250 mm*10 mm) was utilized. The temperature for the test was 150 °C and the solvent was 1,2,4-trichlorobenzene.

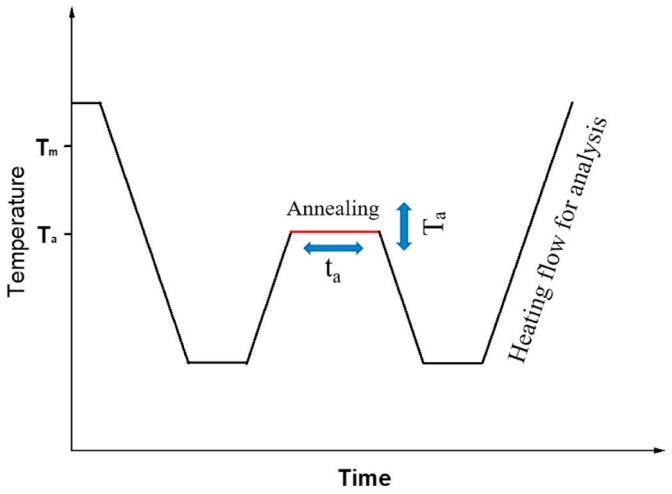

Fig. 1. Procedure of annealing experiments.

2.4.5. Differential scanning calorimeter (DSC)

The melting and crystalline morphologies of POSS/UHMWPE composites were measured by a DSC 3+ instrument (Mettler Toledo, Switzerland). Before measurement, indium (In) was used as a standard medium to calibrate the temperature. The influence of thermal history was excluded by a heating/cooling/reheating sequence. 5–10 mg powder was warmed up and cooled down between 50 and 200 °C at the rate of 10 °C/min, values were recorded for the analysis. All the measurements were conducted under a N_2 atmosphere (50 mL/min).

2.4.6. Fourier transform infrared spectroscopy (FTIR)

The FTIR analysis of POSS/UHMWPE composites was conducted by a Nicolet iS10 fabricated by Thermo Scientific Inc. (Bridgewater NJ, USA). The samples were filmed with KBr, and the measurements were carried out at room temperature.

2.4.7. Scanning electron microscope (SEM)

SEM micrographs were investigated with a Nova Nano 450 to which an energy dispersive X-ray spectrometer (EDS) was linked. The measurements were operated at 10.00 kV. Before the measurement, the samples were kept in an ion-sputtering device to get a thin layer of platinum coating. The device was operated at 120 mA for 60 s.

2.4.8. Transmission electron microscope (TEM)

The dispersion and particle size of POSS domains in the UHMWPE matrix were measured by a transmission electron microscope (TECNAI G2 F20, FEI, USA). Micrographs were analyzed to obtain the particle size of POSS domains.

2.4.9. X-ray diffractometer (XRD)

X-ray diffraction patterns were tested by a diffractometer (D8 Advance, Bruker AXS, Germany) with monochromatized Cu−Kα radiation (λ = 0.154 nm). The samples were measured from 5 to 50° at the rate of 8°/min.

2.4.10. Fast differential scanning calorimeter (Flash-DSC)

A Flash-DSC1 (Mettler-Toledo) was used to study the polymer chain entanglement by annealing test under a nitrogen atmosphere. The samples were warmed up to 165 °C and kept for 5 s to eliminate the thermal history and then cooled to 50 °C for further analysis. Detailed procedure for annealing study is shown in Fig. 1. All the rates here are 100 °C/s.

2.4.11. Mechanical property test

The tensile strength and break elongation of POSS/UHMWPE was evaluated confirming to GB/T 1040.2 with a universal testing machine (MTS Systems, Foshan, China).

Table 2
The influence of POSS on the polymerization catalyzed by Z-N catalyst.[a]

Item	POSS (wt%)	Activity[b]	M_v*10^6 g/mol	MWD
neat UHMWPE	0	15.76	2.7	4.9
0.05% POSS/UHMWPE	0.05	11.32	2.6	5.7
0.1% POSS/UHMWPE	0.1	14.22	2.7	6.2
0.2% POSS/UHMWPE	0.2	11.81	2.6	5.9
0.3% POSS/UHMWPE	0.3	12.99	2.6	5.5
0.4% POSS/UHMWPE	0.4	13.64	2.7	5.5

[a] All reactions were conducted in a 2 L reactor at 85 °C and 0.6 MPa with 1 L purified hexane, [Al]/[Ti] = 150.
[b] Activity: *10^6 g PE*(molTi*h)$^{-1}$.

3. Results and discussion

3.1. Preparation of POSS/UHMWPE nanocomposites

In-situ polymerization was carried out to produce POSS/UHMWPE composites ([Al]/[Ti] = 150, 85 °C). Table 2 shows the polymerization activity with the addition of POSS. Ethylene polymerization is a kind of coordination polymerization and the activation of catalysts requires the complexation between catalyst (Z-N catalyst) and cocatalyst (TEA). The added POSS may hinder the contact between catalysts and cocatalysts, influencing the activation of catalyst. As shown in Table 2, the activity presents a decrease with the addition of POSS. However, no obvious correlation was observed between the activity and the amount of added POSS, some unavoidable reasons such as the fluctuation of temperature can also affect the reaction.

The rheological properties and mechanical properties of polymer depend strongly on its molecular weight. To exclude the effects, the reaction was controlled deliberately and the viscosity average molecular weight (M_v) of synthesized UHMWPE is shown in Table 2. As expected, neat UHMWPE has similar Mv with POSS/UHMWPE composites. Thus, the performance of different samples can be compared [25].

Table 2 also shows the molecular weight distribution (MWD) of POSS/UHMWPE composites measured by a high-temperature GPC. It was found that the MWD of POSS/UHMWPE composite is wider than neat UHMWPE which is beneficial to processing theoretically [26,27].

The identification of POSS in UHMWPE was investigated by SEM-EDS (Fig. 2 (b)). The silicon element provided by the Si-O-Si cage structure of POSS in the matrix is analyzed and identified. The dispersion of POSS in the UHMWPE matrix was measured by TEM and the average particle size was obtained (Fig. 2 (c), (d), Fig. S1). POSS was observed uniformly dispersed in the UHMWPE matrix. From the plot of average particle (domain) size of Fig. 2 (e), it can be concluded that the particle size of POSS domains increased with the increasing POSS content. And when the content is low (<0.3%), the particle size is smaller than the tube size of PE (d_t = 3.26 nm) which may have particular effects on the UHMWPE [11].

The nascent POSS/UHMWPE composites were measured by FT-IR and the spectra are represented in Fig. 3. For comparison, the spectra of neat UHMWPE and POSS are also represented. The FTIR analysis identifies different chemical groups of samples at different wavelengths. The peaks at 1384 cm^{-1} and 1367 cm^{-1} are the characteristic peaks of -CH_3 and -CH_2-, respectively. The relative intensity of the 1384 cm^{-1} band versus the 1367 cm^{-1} band increases with the addition of POSS, revealing that the addition of POSS increases the branching of UHMWPE which can improve the liquidity of UHMWPE [28].

XRD was applied for the measurement of the crystallization of POSS of 2θvalues ranging from 5 to 50° at the scanning rate of 8°/min and the results are shown in Fig. 4. Two main reflections at 21° and 24° were observed and they were associated with the (110) and (200) crystal planes of UHMWPE indicating that POSS did not influence the

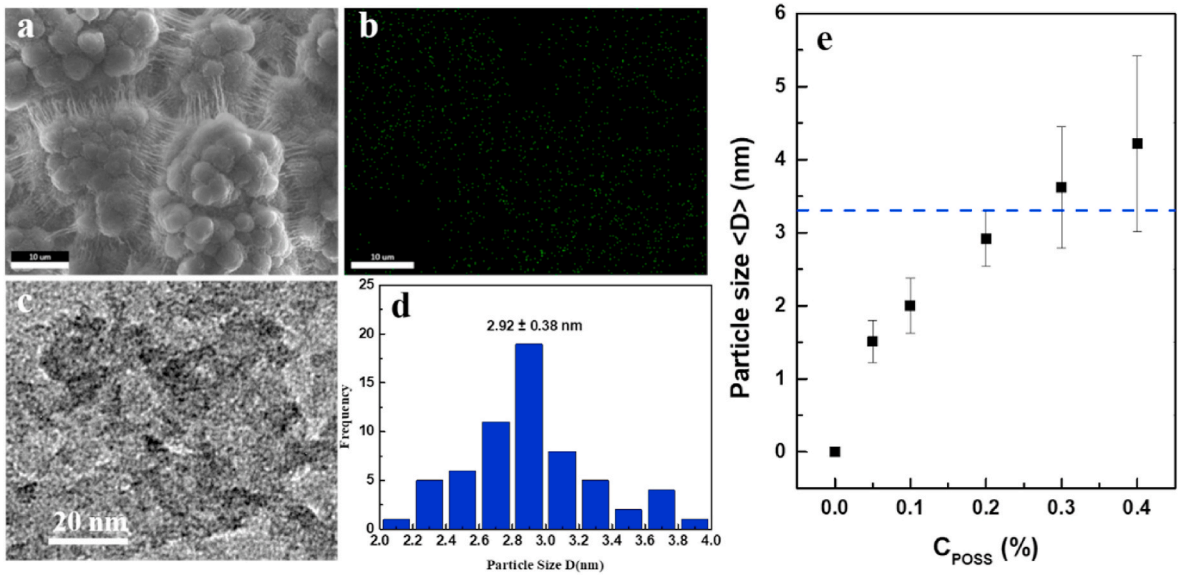

Fig. 2. (a) SEM micrograph of nascent UHMWPE; EDS of (b) 0.2% POSS/UHMWPE (·Si); (c) TEM micrograph of 0.2% POSS/UHMWPE; (d) histogram of particle size of POSS domains of 0.2% POSS/UHMWPE; (e) average nanoparticles size as a function of POSS content in the UHMWPE matrix.

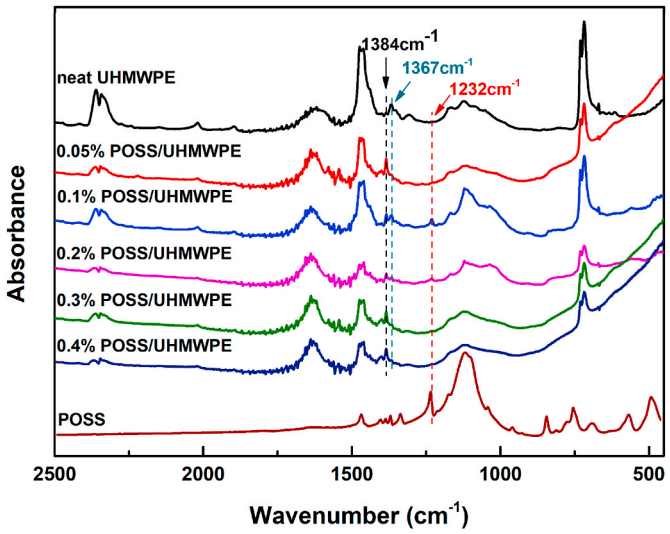

Fig. 3. FTIR spectra of POSS/UHMWPE composites.

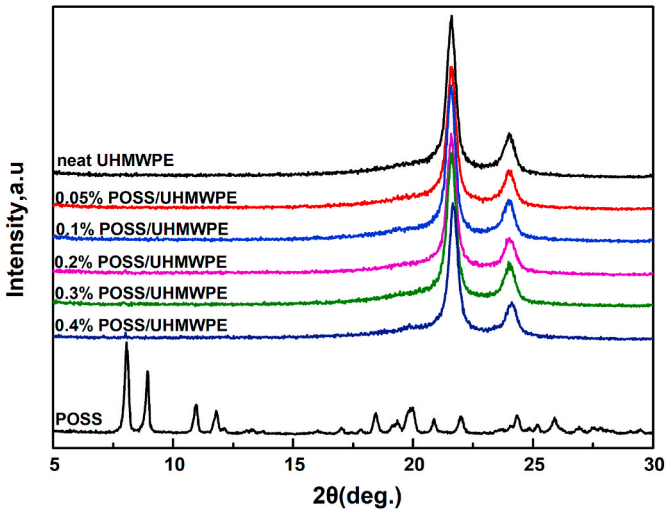

Fig. 4. WAXS intensity traces of POSS/UHMWPE composites.

crystalline structure of UHMWPE [29]. The characteristic peaks of POSS are not observed in POSS/UHMWPE composites with low POSS content, indicating good dispersion of POSS in UHWMPE. When the content is higher, the characteristic peak is recognized, indicating the formation of POSS crystals in UHWMPE matrix [17].

3.2. Thermal transitions

The DSC curves of the first melting and second melting of POSS/UHMWPE composites are shown in Fig. 5. The melting point temperature of the second heating scan is obviously lower than that of the first heating scan, indicating a disentangled structure in the polymers [30]. The detailed results were summarized in Table 3. The melting enthalpy (ΔH_m) was obtained by integrating the melting curves within a certain range (110–150 °C), and the crystallinity (X_c) was summarized by comparing the obtained ΔH_m with the melting enthalpy of perfectly crystallized polyethylene (293 J/g). As has been reported, POSS didn't have impressive effects on the melting and crystallization temperature of UHMWPE [13]. Nevertheless, the addition of POSS increased the melting enthalpy and crystallinity of UHMWPE [25].

3.3. Viscoelastic behavior

Melt viscosity can reflect the entanglement of polyolefin [16]. Generally, the higher entanglement degree can lead to a higher melt viscosity. Small amplitude oscillatory shear measurements (0.01–100 rad/s) were utilized for the measurement of rheological properties of POSS/UHMWPE composites with different POSS contents, which varied from 0.05 to 0.4 wt%. The region of low frequency (0.01–1 rad/s) which is also known as terminal region revealed the small amplitude disturbance to the test system, reflecting the rheological response of UHMWPE matrix chain. More accurate information about the movement of polymer molecular chain can be provided [31]. Fig. 6 shows the dynamic viscosity η* with the decrease of frequency (100–0.01 rad/s) for neat UHMWPE and POSS/UHMWPE composites which was obtained from the equation below:

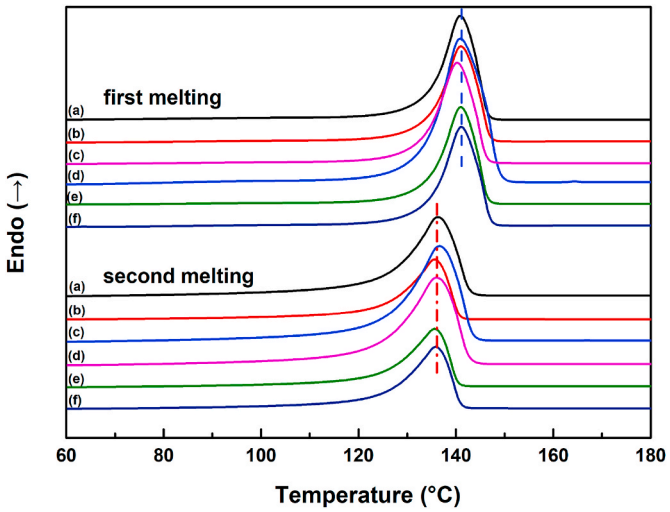

Fig. 5. DSC curves of POSS/UHMWPE composites. (a) neat UHMWPE; (b) 0.05; (c) 0.1; (d) 0.2; (e) 0.3; (f) 0.4 wt% POSS/UHMWPE.

Table 3
Thermal properties of POSS/UHMWPE nanocomposites.

Sample	T_m^1 /°C	T_m^2 /°C	T_c /°C	ΔH_m^1 /Jg^{-1}	X_c^1 /%	ΔH_m^2 /Jg^{-1}	X_c^2 /%
neat UHMWPE	140.9	136.4	120.3	189.2	64.77	129.8	44.29
0.05% POSS/ UHMWPE	141.1	135.5	121.1	194.5	66.37	130.4	44.49
0.1% POSS/ UHMWPE	141.9	136.6	120.3	193.2	65.93	149.3	50.94
0.2% POSS/ UHMWPE	140.2	135.8	119.9	196.0	66.89	145.4	49.64
0.3% POSS/ UHMWPE	141.1	135.5	120.8	190.8	65.10	139.2	47.51
0.4% POSS/ UHMWPE	140.9	135.9	120.8	185.7	63.39	138.1	47.14

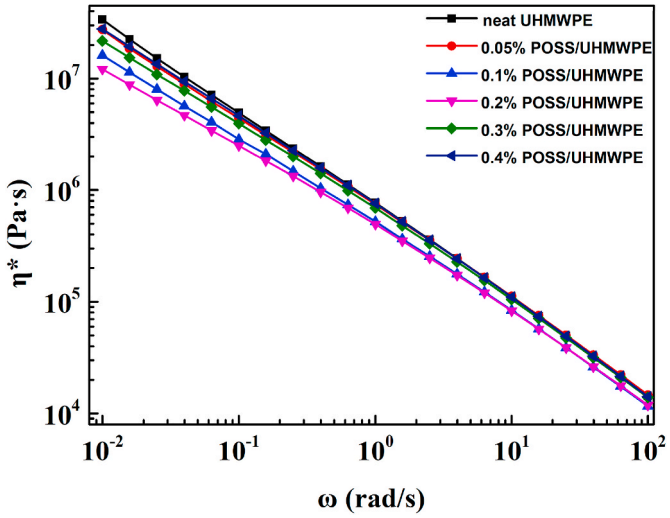

Fig. 6. Melt viscosity of POSS/UHMWPE nanocomposites with different POSS content. T = 180 °C.

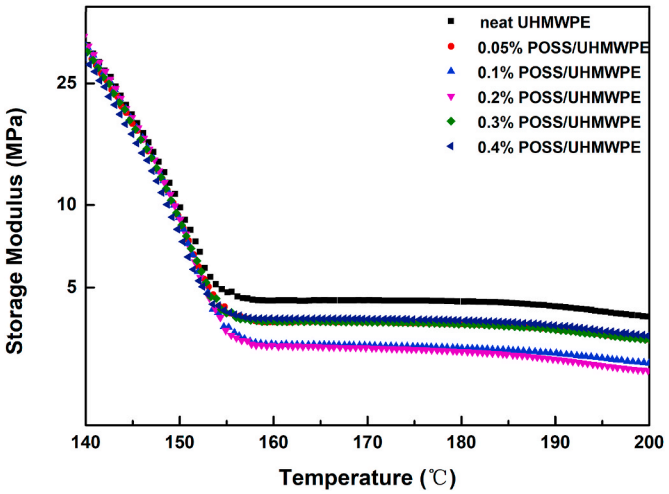

Fig. 7. The storage modulus-temperature curves of neat UHMWPE and POSS/UHMWPE composites.

$$\eta^* = \sqrt{G'^2 + G''^2}\Big/\omega \tag{3}$$

where ω is the frequency of the experiment, G' and G'' are the storage modulus and loss modulus of the samples, respectively. The POSS/UHMWPE melts showed viscosity reduction in the region of low frequency with the addition of POSS. The result is consistent with recent findings that low addition of nanoparticles can lower the melt viscosity of polyolefins [32]. However, because of the increased size of POSS domains, the viscosity increased when the addition increased to 0.3 wt %. Fig. 6 also revealed that the POSS/UHMWPE composites showed shear thinning behavior with the increase of frequency [17]. The reduction of viscosity has been reported to reveal an entanglement expansion mechanism of molecular sliding/lubrication induced by POSS. That is, well dispersed POSS can intercalate the molecular network and induce the increase of free volume, thus reducing the melt viscosity [17].

3.4. Entanglement dilution

The degree of plasticization of polyolefin can be quantified by the molecular weight between entanglement (M_e) figured from rubber platform modulus at thermodynamic equilibrium [33]. The plots of storage modulus-temperature curves of POSS/UHMWPE composites are shown in Fig. 7. The easy formation of a dense entangled network of UHMWPE determines that UHMWPE will not form a traditional continuous melting after heating above the melting point. Therefore, there is a rubber plateau in the temperature range between 160 and 200 °C [13]. The molecular weight (M_e) and density (V_e) between entanglement of UHMWPE can be obtained from equations (4) and (5) [34,35]. M_e is verified as the average molecular weight between two

Table 4
Molecular weight between entanglement (M_e) and entanglement density (V_e) measured from the rubbery plateau region at 190 °C.

Sample	G_N^0 [a]	Me	Ve
neat UHMWPE	4.92	2349.0	367.0
0.05% POSS/UHMWPE	4.04	2859.2	301.5
0.1% POSS/UHMWPE	3.28	3517.3	245.1
0.2% POSS/UHMWPE	3.10	3721.9	231.6
0.3% POSS/UHMWPE	4.04	2860.8	301.3
0.4% POSS/UHMWPE	4.16	2773.7	310.8

[a] G_N^0: equilibrium modulus at 190 °C.

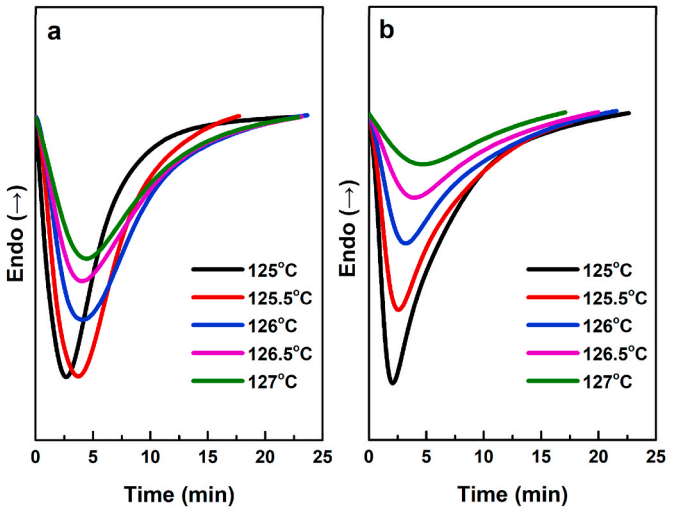

Fig. 8. DSC curves of the isothermal crystallization of POSS/UHMWPE composites at different crystallization temperatures: (a) neat UHMWPE; (b) 0.2% POSS/UHMWPE.

entanglement nodes in the chain of UHMWPE, and V_e is verified as the proportion of the number of instantaneous entanglement points to the average number of entanglement points in the equilibrium state.

$$M_e = \frac{3\rho RT}{E_e} \tag{4}$$

$$V_e = \frac{\rho}{M_e} \tag{5}$$

where ρ is the density of the composites and is equal to 0.862 g/cm^3, R is the universal gas constant (8.314 Jmol^{-1}K^{-1}), T is the absolute temperature. E_e is the storage modulus in the thermodynamic equilibrium state measured by DMA in tensile mode [36].

The specific values of M_e and V_e are summarized in Table .4. It is suggested that POSS could intercalate the entanglement network when its domain size is smaller than the tube diameter of polyethylene (d_t, ca.3.28 nm). When the content of POSS is small (0.05–0.2 wt%), M_e of the composites increased and V_e decreased, revealing that POSS can definitely diminish the entanglement of UHMWPE. When the addition comes to 0.3 wt%, POSS tends to agglomerate and the size of the domains becomes larger than d_t, Thus the M_e decreased and V_e increased [37]. The results reflected the influence of the size of POSS domains on the polymer dynamics and the trend of M_e and V_e is consistent with the results of complex viscosity (η*) discussed above.

3.5. Isothermal crystallization analysis

DSC instrument was utilized for the investigation of the isothermal crystallization behaviors of POSS/UHMWPE composites. The crystalline ability of the polymer chains was quantitatively studied. The Avrami equation is always applied for the study of isothermal crystallization kinetics [38]:

$$X_t = 1 - exp[-Z_t t^{n_a}] \tag{6}$$

where Z_t is the rate constant of Avrami crystallization, n_a is the exponent associated with the mechanism of nucleation.

Typical isothermal crystallization curves of POSS/UHMWPE composites of different crystallization temperatures are represented in Fig. 8. It can be concluded that the exothermic peak of the curve shifts to the right with the increase of the isothermal crystallization temperature, indicating that the required time for UHMWPE to complete crystallization was increased. X_t is the corresponding crystallinity at time t which is

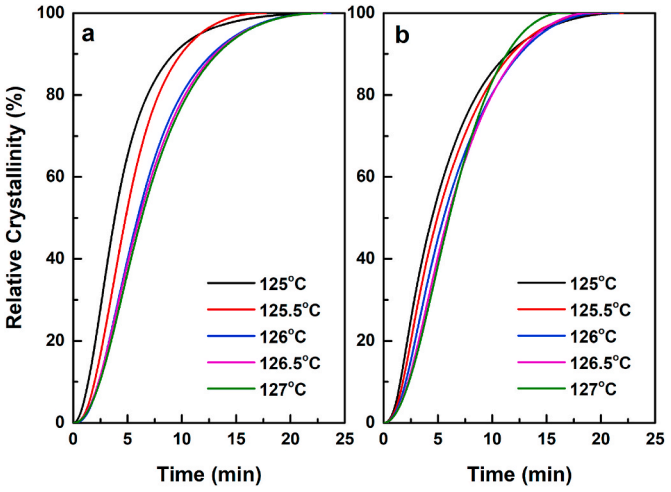

Fig. 9. Development of X_t with the crystallization time for the isothermal crystallization of (a) neat UHMWPE; (b) 0.2% POSS/UHMWPE.

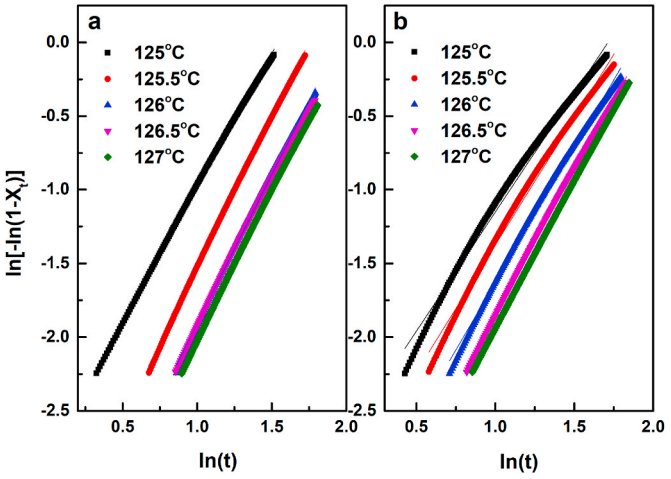

Fig. 10. Plots of ln[-ln(1-X_t)] verses ln(t) for (a) neat UHMWPE and (b) 0.2% POSS/UHMWPE during isothermal crystallization.

Table 5
Parameters of isothermal crystallization kinetics of POSS/UHMWPE composites.

Sample	T(°C)	Z_t(min^{-1})	$t_{1/2}$[a]	$t_{1/2}$[b]	n	$\bar{n}$
neat UHMWPE	125	0.061	3.82	3.80	1.82	1.97
	125.5	0.028	4.8	4.82	2.04	
	126	0.020	5.9	5.78	2.02	
	126.5	0.021	6.07	5.95	1.96	
	127	0.018	6.27	6.21	2	
0.2% POSS/UHMWPE	125	0.063	4.45	4.43	1.61	1.81
	125.5	0.045	4.93	4.9	1.72	
	126	0.031	5.5	5.46	1.83	
	126.5	0.023	5.9	5.84	1.93	
	127	0.020	6.03	5.99	1.98	

[a] determined from Fig. 10. (min).
[b] calculated from Avrami equation (min).

calculated as below:

$$X_t = \frac{X_t(t)}{X_t(\infty)} = \frac{\int_0^t (dH(t)/dt)dt}{\int_0^\infty (dH(t)/dt)dt} \tag{7}$$

where $dH(t)/dt$ is the rate of heat flow, $X_t(t)$ and $X_t(\infty)$ are the crystallinity at time t, and the crystallinity of the completed crystallization

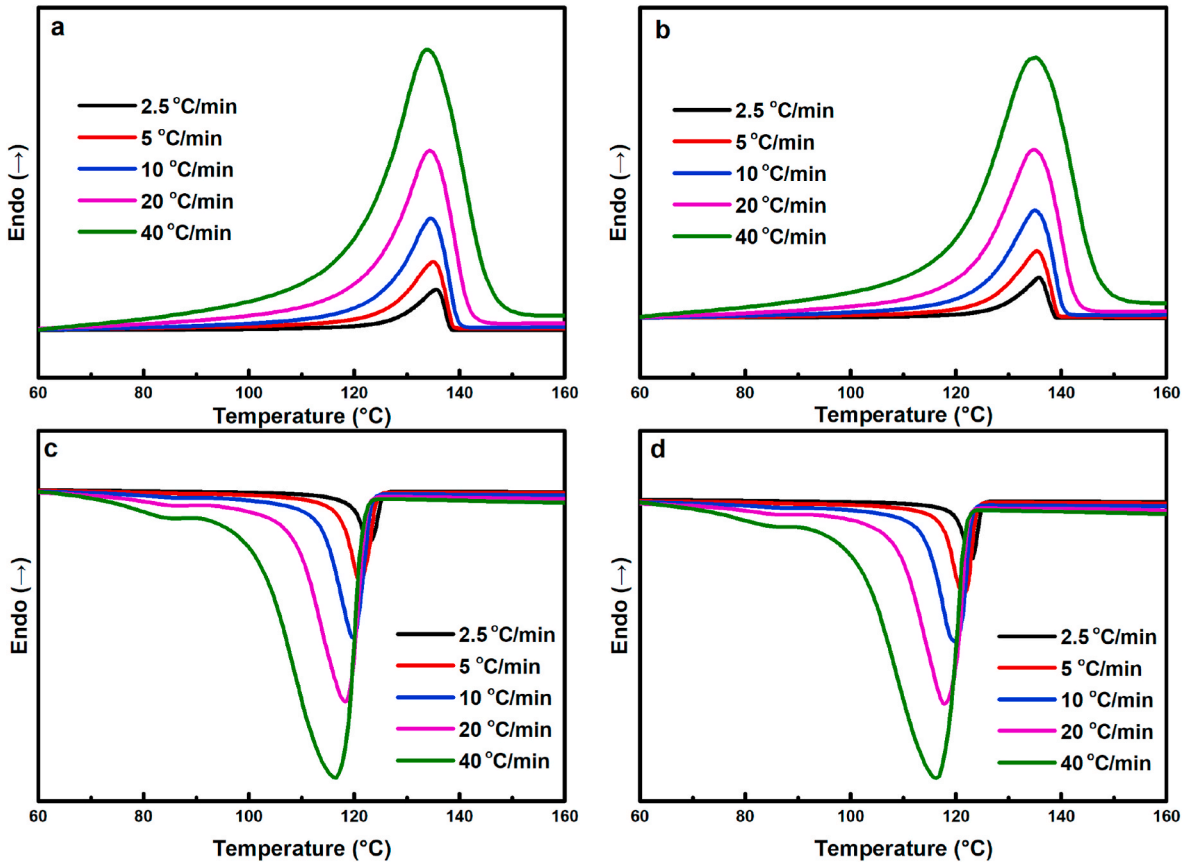

Fig. 11. DSC curves at different rates: heating scan of (a) neat UHMWPE, (b) 0.2% POSS/UHMWPE; cooling scan of (c) neat UHMWPE, (d) 0.2% POSS/UHMWPE.

process, respectively. Thus, the development of X_t as the function of the crystallization time for UHMWPE was presented (Fig. 9).

$$ln[-ln(1-X_t)] = lnZ_t + nlnt \tag{8}$$

Plots of ln[-ln(1-X_t)] verses ln(t) for POSS/UHMWPE composites during isothermal crystallization were obtained in Fig. 10. Half time of crystallization ($t_{1/2}$) of a polymer is assumed as a measure of the comprehensive crystallization rate. It can be directly obtained from Fig. 9 or calculated from equation (9):

$$t_{1/2} = \left(\frac{ln2}{Z_t}\right)^{1/n} \tag{9}$$

The fitting results of the isothermal crystallization are summarized in Table 5. The $t_{1/2}$ of both neat UHMWPE and 0.2% POSS/UHMWPE increased with the increase of T_c, revealing that the crystallization occurs by a nucleation-controlled mechanism [25]. There are few deviations between the experimental data and the calculated data, indicating that Avrami equation can well illustrate the isothermal crystallization of UHMWPE. The Z_t of neat UHMWPE and 0.2% POSS/UHMWPE are all close to 2, indicating the concurrent emergency of two-dimensional crystal growth with heterogeneous nucleation [39]. Uniformly dispersed POSS could induce heterogeneous nucleation of UHMWPE and the effects become obvious when the isothermal crystallization temperature gets higher. The crystallization rate indicated by $t_{1/2}$ reveals that the addition of POSS could accelerate the crystallization rate when the isothermal crystallization temperature is higher and this is consistent with the trend of heterogeneous nucleation. It can be concluded that POSS acted as a nucleation agent for the initial nucleation and pursuant growth of the crystals.

Table 6
Non-isothermal crystallization parameters of neat UHMWPE and 0.2% POSS/UHMWPE.

Sample	Φ (°C/min)	T_0 (°C)	T_c (°C)	$t_{1/2}$ (s)	ΔH_m (J/g)	X_c (%)
neat UHMWPE	2.5	126.5	122.7	117	139.2	47.5
	5	126.2	121.1	70	131.3	44.8
	10	125.2	119.8	45	123.8	42.3
	20	124.7	118.3	30	118.4	40.4
	40	124.1	116.6	19	116.3	39.7
0.2% POSS /UHMWPE	2.5	126.4	122.8	96	151.4	51.7
	5	125.5	121.4	63	146.7	50.1
	10	124.7	119.8	41	138.3	47.2
	20	124.1	117.8	28	131.0	44.7
	40	123.5	116.2	18	127.9	43.7

Φ = heating rate and cooling rate; T_0 = starting crystallization temperature; T_c = crystallization temperature.

3.6. Nonisothermal crystallization analysis

Compared with isothermal crystallization, the nonisothermal crystallization process is closer to the actual processing of the polymer, so the investigation of nonisothermal behavior and kinetics can play an important role in the industrial production of UHMWPE.

The nonisothermal melt crystallization exotherms at different cooling rates are represented in Fig. 11. The exothermic traces became wider and shifted to lower temperature as the cooling rate increased for all samples, indicating that the crystallization was governed by the nucleation rate [40]. The parameters of nonisothermal crystallization are summarized in Table 6. It was shown that with the addition of POSS, the crystallinity determined by the enthalpy of melting was increased, and the crystallization rate determined by $t_{1/2}$ (Fig. 12) was increased, revealing that POSS can act as nucleus for UHMWPE.

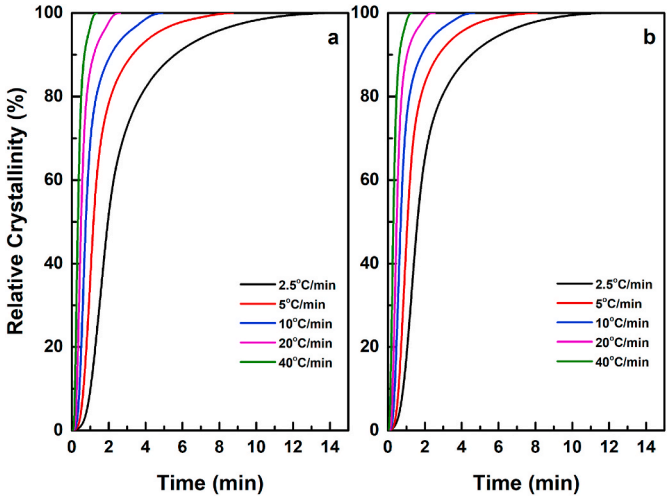

Fig. 12. Development of X_t with the crystallization time for the non-isothermal crystallization of (a) neat UHMWPE; (b) 0.2% POSS/UHMWPE.

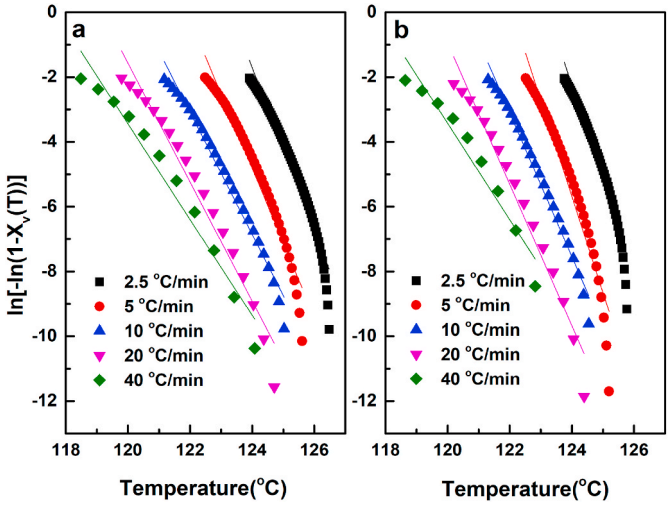

Fig. 13. Plots of ln[-ln(1-X_v(T))]-T of (a) neat UHMWPE and (b) 0.2% POSS/UHMWPE with different POSS content during non-isothermal crystallization.

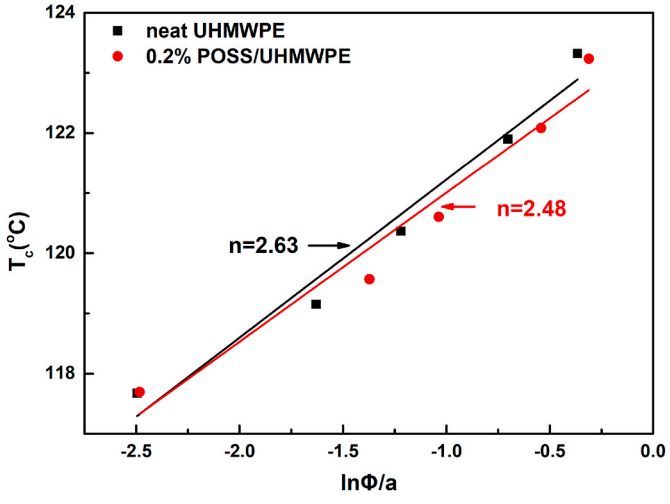

Fig. 14. Plot of T_c versus lnφ/a for neat UHMWPE and 0.2% POSS/UHMWPE.

Table 7
The non-isothermal crystallization kinetics parameters of neat UHMWPE and 0.2% POSS/UHMWPE.

Sample	Φ (°C/min)	T_c^a (°C)	T_c^b (°C)	a	n
neat UHMWPE	2.5	122.7	123.3	−2.5	2.62
	5	121.1	121.9	−2.3	
	10	119.8	120.4	−1.9	
	20	118.3	119.2	−1.8	
	40	116.6	117.7	−1.5	
0.2% POSS /UHMWPE	2.5	122.8	123.2	−2.9	2.48
	5	121.4	122.1	−2.9	
	10	119.8	120.6	−2.2	
	20	117.8	119.6	−2.2	
	40	116.2	117.7	−1.5	

When the cooling rate increased, the difference of $t_{1/2}$ of the two samples became smaller. That phenomenon results from the ultrahigh molecular weight of UHMWPE. When the rate is small, there is enough time for the rearrangement of molecular chain of UHMWPE during the process and crystallization, so the crystallization rate varies greatly. When the rate gets higher, the linear unbranched molecular chain of UHMWPE crystallizes very quickly, the chain does not have enough time to rearrange.

The Ozawa method was applied to investigate the nonisothermal crystallization behavior. The Ozawa plots of neat UHMWPE and 0.2% POSS/UHMWPE were shown in Fig. 13.

$$ln[-ln(1-X_v(T))] = a(T-T_q) \tag{10}$$

where T_q is the crystallization peak temperature; $X_v(T)$ is the volume fraction of polymer at crystallization temperature T which can be determined from the equation below:

$$X_v(T) = \frac{X_w(T)\frac{\rho_a}{\rho_c}}{1-\left(1-\rho_a/\rho_c\right)X_w(T)} \tag{11}$$

where ρ_a and ρ_c equal to the density of amorphous and crystalline phase of UHMWPE, and $\rho_a = 0.865$, $\rho_c = 1.000$. As can be seen, the results show a good linear relationship. The parameters a and -aT_q can be calculated from the slope and intercept of the fitting curve.

The plot of lnΦ/a verses T_q is shown in Fig. 14.

$$T_q = nln\varphi/a + b \tag{12}$$

From the plot of the fitting curve, the parameter of Avrami - n can be obtained (Table 7): 2.62 for neat UHMWPE, 2.45 for 0.2% POSS/UHMWPE, indicating they have the same crystallization type. The non-integer form of the Avrami index may be caused by factors such as the secondary crystallization process, the mixing nucleation method, and the density change of the material.

3.7. Annealing study

The thermal history of polymers domains its melting behavior strongly [41,42]. A flash-DSC was utilized for the annealing experiments under different annealing times and temperatures to explore the effects of POSS on the entanglement of UHMWPE. It was reported that the successive peeling of the chains from the crystal substrate occurs during the annealing process, and a new crystal state can be formed when the sample was cooled down, causing difference in the melting behavior [43]. As can be seen from Fig. 15, two obvious endothermic peaks were inspected after annealing. It was reported that the extra melting peak was resulted from the sectional melting and recrystallization during annealing [41]. As has been reported, the endothermic peak at lower temperature is associated with the crystals formed by secondary crystallization, while the endothermic peak at higher temperature is

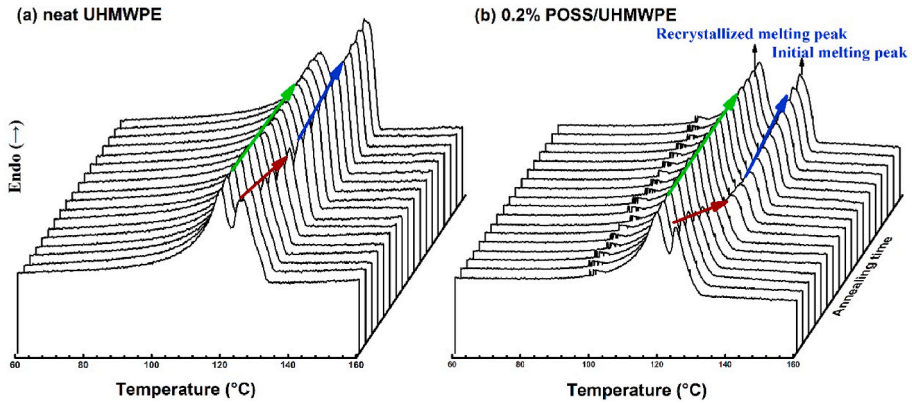

Fig. 15. The DSC curves of (a) neat UHMWPE and (b) 0.2% POSS/UHMWPE in different annealing time. (T_a = 121 °C).

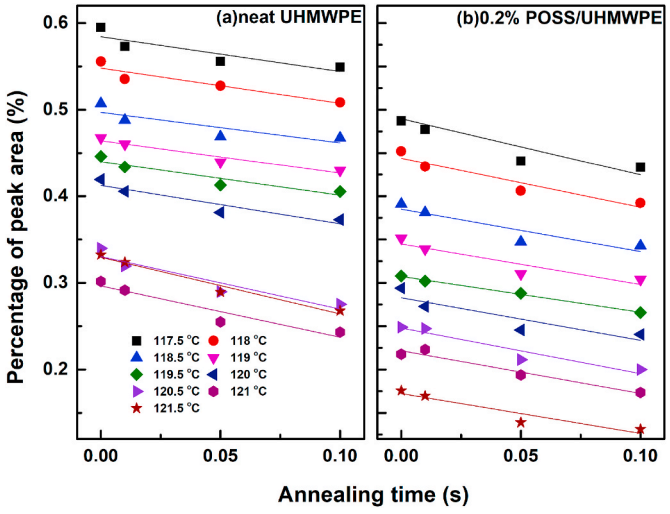

Fig. 16. The decrease in the relative area of the high temperature melting peak of (a) neat UHMWPE and (b) 0.2% POSS/UHMWPE for different annealing times at different annealing temperatures.

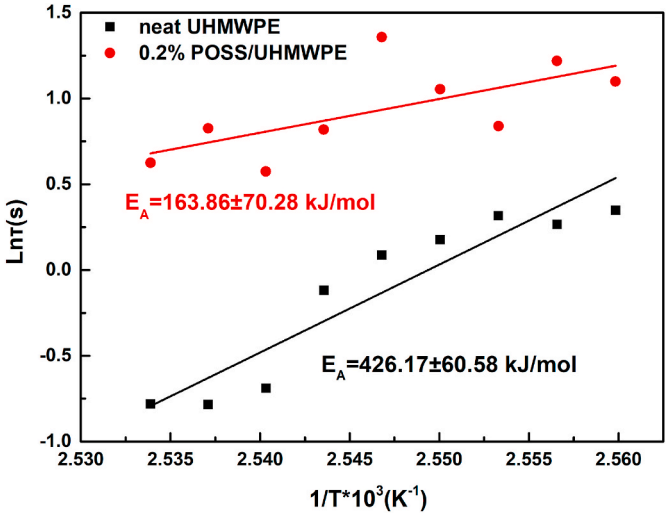

Fig. 17. Influence of POSS on melt activation energy during annealing.

associated with the crystals formed from initial crystallization [43].

With the addition of annealing time, the melting peaks of higher temperature were shifted to higher temperature, and the melting peaks of lower temperature were shifted to lower temperature, increasing the temperature difference between them. This indicates that with the extension of annealing time, the partial melting and recrystallization were gradually perfected. When the annealing time was short (<0.1s), the proportion of the peak area of the recrystallized melting peak to that of the initial melting peak increased. This may be mainly because as the annealing time increases, more polymer chains could fall off from the matrix and recrystallized [13]. Thus, the recrystallized part increased and the primary crystallized part decreased. It was reported that the disentangled UHMWPE possesses higher local mobility [41,42]. As can be seen, under the same annealing time, the peak area ratio of the recrystallized melting peak to the initial melting peak of POSS/UHMWPE is higher than that of neat UHMWPE, indicating that the added POSS improves the capacity of chain diffusion and has specific effects on the disentanglement of UHWMPE.

However, when the annealing time was longer (>0.1s), the peak area of initial melting peak increased. As has been reported, the fraction of free volume in polymers increases firstly and then decreases with the increase of its annealing time [44]. So, it can be speculated that when the annealing time increases, the free volume of UHMWPE decreases which limits the movement of the chain.

3.8. Segment dynamic of POSS/UHMWPE composites

The areas of the two melting peaks discussed above is proportional to the amount of corresponding crystals, so the proportion of the peak areas can be the measurement for the ratio of the amounts of corresponding crystals formed by recrystallization or in the initial nascent state [43]. As has been discussed, when the annealing reached a certain level, the slip diffusion of the chain segment gradually slows down and stops. The slip and diffusion of the chain segments at the beginning of annealing can better reflect the movement of the UHMWPE molecular chains. The annealing experiments were carried out from 118.5 to 121.5 °C. Fig. 16 shows that the normalized initial melting enthalpy decreased with the extension of annealing time and temperature increased, revealing that more polymer chains detached from the matrix as the annealing time and temperature increased. Moreover, the percentages of the POSS/UHMWPE composite are evidently smaller than those of neat UHMWPE, indicating that POSS has impressive influence on the disentanglement.

The flexibility of polymers is closely related to the melting behavior of polymers. The enthalpic relaxation times for different melt processes can be determined by Fig. 17 with Debye (Arrhenius) equation [13,43].

$$H(T,t) = H_0(T)e^{-t/\tau(T)} \tag{13}$$

Among them, τ(T) is the time constant, T and t are the annealing temperature and annealing time, respectively. Because of the enthalpy loss caused by Flash DSC, the parameter "a" was introduced. The

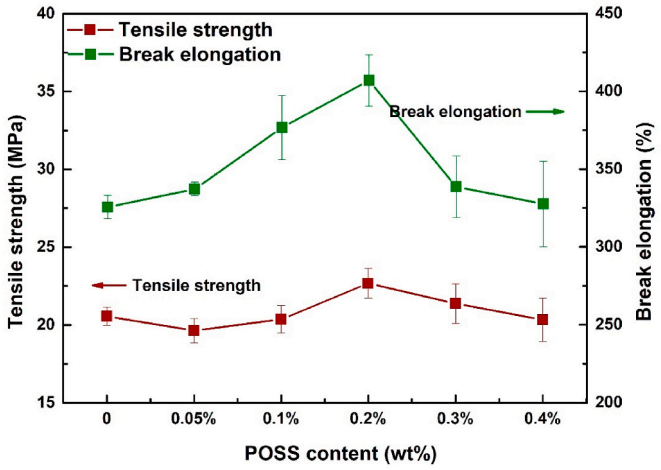

Fig. 18. Machenical properties of POSS/UHMWPE composites.

relationship between the time constant (τ) and the activation energy (E_A) can be determined by

$$\tau = \tau_0 e^{E_A/RT} \tag{14}$$

The time constant (τ) of various temperatures can be obtained from Fig. 17 with equation (13). The plot of ln τ as a function of 1/T is shown in Fig. 17, two curves with different slopes were obtained. From equation (14), the melt activation energy can be attained from the fitting slopes [43]. The obtained melt activation energies are 426.17± 60.58 kJ/mol for neat UHWMPE and 163.86 ± 70.28 kJ/mol for POSS/UHMWPE composite. The obtained melt activation energies are attributed to the energy barriers that the chain segments must overcome to detach from the crystal and then diffuse into the melt. The POSS/UHMWPE composite has a lower activation energy, revealing that it requires lower energy for the chain segment to move and melt. The lowered melt activation energies in POSS/UHMWPE composites would have the potential to benefit the use of PE in thermal sealing applications involving packaging.

3.9. Mechanical study

The influence of POSS on the tensile strength and break elongation of UHMWPE was also investigated, and the results are summarized in Fig. 18. It shows that POSS didn't show outstanding influence on the tensile strength of UHMWPE. However, obvious effects were observed on the break elongation. With the addition of POSS, the break elongation increased, and it reached the maximum when the content was 0.2 wt% with an increase of 94.8%. When the content was further increased, the break elongation decreased instead. Same mechanical reinforcements were also shown in POSS/PE films that their mechanical properties increased at low concentration of POSS while decreases at higher concentration of POSS [15]. The volume control of POSS domains is responsible the phenomenon. When the size of POSS domains is small (<tube diameter of polyethylene), POSS intercalates the molecular chain and acts as a physical crosslink to prevent the sliding and alignment of the polyethylene chains during extensional flow. At higher POSS content, the size of POSS domains increased due to agglomeration, and reduced mechanical properties are observed because POSS acts as stress concentrator in the UHMWPE matrix.

4. Conclusion

Soluble POSS was added in UHMWPE by in-situ polymerization to avoid the agglomeration. The influence of POSS on the polymerization, dispersion, thermal transitions, melt viscosity, crystallization behavior, annealing behavior and mechanical properties were investigated. The addition of POSS affected the activation of Z-N catalysts and widen the molecular weight distribution which is beneficial to processing. TEM spectra of nascent POSS/UHMWPE composites show uniform dispersion of POSS in UHMWPE matrix and the particle size of POSS domains increased as the POSS content increased. The melt viscosity of POSS/UHMWPE composites decreased with the addition of POSS and the optimum content is 0.2 wt%. The rubbery plateau modulus of UHMWPE was remarkably decreased with the introduction of POSS, indicating a strong dilation effect of POSS on polymer entanglements. The crystallization study of POSS/UHMWPE composites indicated that uniformly dispersed POSS can induce heterogeneous crystallization of UHMWPE, accelerate the crystallization rate and increase the crystallinity. A Flash DSC was utilized for the annealing study of the composites. The percentage of re-crystallized melting peak area of POSS/UHMWPE composite is higher than that of neat UHMWPE, revealing more polymer chains detached from the matrix during annealing. The melt activation energies of neat UHMWPE and POSS/UHMWPE composite were calculated by Arrhenius equation and the results show that the added POSS can impressively diminish the energy barrier of the polymer chains during annealing, reflecting impressive effects of POSS on the disentanglement of UHMWPE.

CRediT authorship contribution statement

Jian Zhou: Methodology, Software, Validation, Formal analysis, Investigation, Data curation, Project administration, Writing – original draft, Visualization, Conceptualization. **Xian Zhang:** Investigation, Writing – review & editing. **Shicheng Zhao:** Resources, Project administration, Writing – review & editing, Supervision. **Chunlin Ye:** Methodology, Investigation. **Zhenfei Zhang:** Methodology, Investigation. **Shiao-Wei Kuo:** Investigation, Supervision. **Zhong Xin:** Conceptualization, Supervision, Resources, Project administration, Writing – review & editing, Funding acquisition.

Declaration of competing interest

The authors declare that they have no known competing financial interests or personal relationships that could have appeared to influence the work reported in this paper.

Acknowledgements

This work was financially supported by National Natural Science Foundation of China (Grant 22178108).

Appendix A. Supplementary data

Supplementary data to this article can be found online at https://doi.org/10.1016/j.polymer.2022.124561.

References

[1] S.L. Liu, J.Y. Chen, Y. Cao, Effect of solid paraffin on the integrity of welded interfaces and properties of ultra-high molecular weight polyethylene, Polym. Sci. 57 (2015) 168–176.
[2] D. Barron, C. Birkinshaw, Ultra-high molecular weight polyethylene - evidence for a three-phase morphology, Polymer -London 49 (5) (2008) 3111–3115.
[3] P. Chammingkwan, Y. Bando, L.T.T. Mai, T. Wada, A. Thakur, M. Terano, L. Sinthusai, T. Taniike, Less entangled ultrahigh-molecular-weight polyethylene produced by nano-dispersed Ziegler–natta catalyst, Ind. Eng. Chem. Res. 60 (7) (2021) 2818–2827.
[4] W. Li, Z. Yue, A. Lozovoi, O. Petrov, C. Mattea, S. Stapf, Heterogeneous distribution of chain mobility in nascent UHMWPE in the less entangled state, J. Polym. Res. 25 (11) (2018) 239.
[5] A. Osichow, C. Rabe, K. Vogtt, T. Narayanan, L. Harnau, M. Drechsler, M. Ballauff, S. Mecking, Ideal polyethylene nanocrystals, J. Am. Chem. Soc. 135 (31) (2013) 11645–11650.

[6] V.M. Litvinov, M.E. Ries, T.W. Baughman, A. Henke, P.P. Matloka, Chain entanglements in polyethylene melts. Why is it studied again? Macromolecules 46 (2) (2013) 541–547.
[7] S. Rastogi, D. Lippits, G. Peters, R. Graf, Y. Yao, H. Spiess, Heterogeneity in polymer melts from melting of polymer crystals, Nat. Mater. 4 (8) (2005) 635–641.
[8] W. Li, C. Guan, J. Xu, J. Mu, D. Gong, Z.R. Chen, Q. Zhou, Disentangled UHMWPE/POSS nanocomposites prepared by ethylene in situ polymerization, Polymer 55 (7) (2014) 1792–1798.
[9] W. Li, L. Hui, B. Xue, C. Dong, Y. Chen, L. Hou, B. Jiang, J. Wang, Y. Yang, Facile high-temperature synthesis of weakly entangled polyethylene using a highly activated Ziegler-Natta catalyst, J. Catal. 360 (2018) 145–151.
[10] Z. Yue, N. Wang, Y. Cao, W. Li, C. Dong, Reduced entanglement density of ultra-high molecular weight polyethylene favored by the isolated immobilization on MgCl2(110) plane, Ind. Eng. Chem. Res. 59 (8) (2020) 3351–3358.
[11] R. Mangal, S. Srivastava, S. Narayanan, L.A. Archer, Size-dependent particle dynamics in entangled polymer nanocomposites, Langmuir 32 (2) (2016) 596–603.
[12] K. Liu, E.D. Boer, Y. Yao, D. Romano, S. Ronca, S. Rastogi, Heterogeneous distribution of entanglements in a nonequilibrium polymer melt of UHMWPE: influence on crystallization without and with Graphene Oxide, Macromolecules 49 (19) (2016) 7497–7509.
[13] X. Zhang, S. Zhao, Z. Xin, The chain dis-entanglement effect of polyhedral oligomeric silsesquioxanes (POSS) on ultra-high molecular weight polyethylene (UHMWPE), Polymer 202 (2020), 122631.
[14] M. Mohamed, K. Shiao-Wei, Polybenzoxazine/Polyhedral oligomeric silsesquioxane (POSS) nanocomposites, Polymers 8 (6) (2016) 225.
[15] A. Romo-Uribe, J. Lichtenhan, A. Reyes-Mayer, M. Calixto-Rodriguez, E. Sarmiento-Bustos, M. Yanez-Lino, Parts-per-million polyhedral oligomeric silsesquioxane loading induced mechanical reinforcement in polyethylene nanocomposites. When small and well-dispersed yields big, Polym. Adv. Technol. 31 (11) (2020) 2453–2465.
[16] M. Guo, É. David, M. Fréchette, N.R. Demarquette, Polyethylene/polyhedral oligomeric silsesquioxanes composites: dielectric, thermal and rheological properties, Polymer 115 (2017) 60–69.
[17] Romo-Uribe Angel, Reyes-Mayer Adriana, Paredes-Pérez Marcela, Lichtenhan Joseph, Mauricio, POSS driven chain disentanglements, decreased the melt viscosity and reduced O2 transmission in polyethylene, Polymer (2019) 61–71.
[18] R.U. Angel, Viscoelasticity and microstructure of POSS-methyl methacrylate nanocomposites. Dynamics and entanglement dilution, Polymer 148 (2018) 27–38.
[19] A. Romo-Uribe, J.D. Lichtenhan, Melt extrusion and blow molding parts-per-million POSS interspersed the macromolecular network and simultaneously enhanced thermomechanical and barrier properties of polyolefin films, Polym. Eng. Sci. 61 (1) (2020) 245–257.
[20] Y. Yang, H. Xu, H. Gu, Preparation and crystallization of poly(ethylene terephthalate)/SiO2 nanocomposites by in-situ polymerization, J. Appl. Polym. Sci. 102 (1) (2006) 655–662.
[21] A. Romo-Uribe, Dispersion at single unit TiO2 nanoparticles reduced Tg, induced chain disentanglement and reduced tensile modulus in waterborne acrylic coatings, Macromol. Mater. Eng. 306 (2021), 2000519.
[22] J. Rong, Z. Jing, H. Li, S. Miao, A polyethylene nanocomposite prepared via in-situ polymerization, Macromol. Rapid Commun. 22 (5) (2001) 329–334.
[23] A. Arzac, G.P. Leal, R. Fajgar, R. Tomovska, Comparison of the emulsion mixing and in situ polymerization techniques for synthesis of water-borne reduced Graphene oxide/polymer composites: advantages and drawbacks, Part. Part. Syst. Char. 31 (1) (2014) 143–151.
[24] B. Standards, Plastics - Determination of the Viscosity of Polymers in Dilute Solution Using Capillary Viscometers - Part 3: Polyethylenes and Polypropylenes.
[25] G. Chao, H. Yang, L. Wei, D. Zhou, Z.e. Chen, Crystallization behavior of ultrahigh-molecular-weight polyethylene/polyhedral oligomeric silsesquioxane nanocomposites prepared by ethylene in situ polymerization, J. Appl. Polym. Sci. 131 (19) (2014), 40847.
[26] B. Zhang, X. Qiao, Z. Liu, C.Y. Liu, Molecular Weight And Molecular Weight Distribution Determination Of Uhmwpe From Rheological Methods, 2011.
[27] J.E. Jam, M. Nekoomanesh, M. Ahmadi, H. Arabi, From molecular weight distribution to linear viscoelastic properties and back again: application to some commercial high-density polyethylenes, Iran. Polym. J. (Engl. Ed.) 21 (6) (2012) 403–413.
[28] S. Yang, Determination Of Methyl (Comonomer) Content In Polyethylene By Fourier Transform Infrared Spectrophotometry (Ft-Ir), Infrared, 2005, pp. 9–14.
[29] T.G. Gopakumar, J.A. Lee, M. Kontopoulou, J.S. Parent, Influence of clay exfoliation on the physical properties of montmorillonite/polyethylene composites, Polymer 43 (20) (2002) 5483–5491.
[30] M. Hikosaka, K. Amano, S. Rastogi, A. Keller, Lamellar thickening growth of an extended chain single crystal of polyethylene (II): ΔT dependence of lamellar thickening growth rate and comparison with lamellar thickening, J. Mater. Sci. 35 (20) (2000) 5157–5168.
[31] H. Wang, X. Yang, Z. Fu, X. Zhao, Y. Li, J. Li, Rheology of nanosilica-compatibilized immiscible polymer blends: formation of a "heterogeneous network" facilitated by interfacially anchored hybrid nanosilica, Macromolecules 50 (23) (2017) 9494–9506.
[32] N. Shi, J. Han, L. Ni, A. Zheng, Preparation and rheological characterization of ultra high molecular weight polyethylene/montmorillonite nanocomposites, J. Macromol. Sci. Part D - Rev. Polym. Process. 49 (3) (2010) 292–295.
[33] D. Kim, S. Srivastava, S. Narayanan, L.A. Archer, Polymer nanocomposites: polymer and particle dynamics, Soft Matter 8 (42) (2012) 10813–10818.
[34] M. Xie, H. Li, Viscosity reduction and disentanglement in ultrahigh molecular weight polyethylene melt: effect of blending with polypropylene and poly(ethylene glycol), Eur. Polym. J. 43 (8) (2007) 3480–3487.
[35] D.R. Lippits, S. Rastogi, S. Talebi, C. Bailly, Formation of entanglements in initially disentangled polymer melts, Macromolecules 39 (26) (2006) 8882–8885.
[36] R.M. Gul, F.J. Mcgarry, Processing of ultra-high molecular weight polyethylene by hot isostatic pressing, and the effect of processing parameters on its microstructure, Polym. Eng. Sci. 44 (10) (2004) 1848–1857.
[37] P.J. Jones, R.D. Cook, C.N. Mcwright, R.J. Nalty, V. Choudhary, S.E. Morgan, Polyhedral oligomeric silsesquioxane–polyphenylsulfone nanocomposites: investigation of the melt-flow enhancement, thermal behavior, and mechanical properties, J. Appl. Polym. Sci. 121 (5) (2011) 2945–2956.
[38] H.M. Hulburt, J.O. Hirschfelder, Potential energy functions for diatomic molecules, J. Chem. Phys. 9 (1) (1941) 61–69.
[39] M. Trujillo, M.L. Arnal, A. Müller, E. Laredo, S. Bredeau, D. Bonduel, P. Dubois, Thermal and morphological characterization of nanocomposites prepared by in-situ polymerization of high-density polyethylene on carbon nanotubes, Macromolecules 40 (17) (2007) 6268–6276.
[40] A.R. Adhikari, K. Lozano, M. Chipara, Non-isothermal crystallization kinetics of polyethylene/carbon nanofiber composites, J. Compos. Mater. 46 (7) (2012) 823–832.
[41] Y. Kong, J.N. Hay, Multiple melting behaviour of poly(ethylene terephthalate), Polymer 44 (3) (2003) 623–633.
[42] D.R. Lippits, S. Rastogi, G.H. Hne, B. Mezari, P. Magusin, Heterogeneous distribution of entanglements in the polymer melt and its influence on crystallization, Macromolecules 40 (4) (2007) 1004–1010.
[43] S. Rastogi, D.R. Lippits, G.H. Hne, B. Mezari, P. Magusin, The role of the amorphous phase in melting of linear UHMW-PE; implications for chain dynamics, J. Phys. Condens. Matter 19 (20) (2007), 205122.
[44] S. Shen, J. Lou, J. Cheng, K. Hong, Q. Zhu, X. Zhou, Studies on the free-volume change in annealed ultra-high-molecular-weight polyethylene by the positron-annihilation technique, Phys. Status Solidi 147 (2) (2010) 447–452.